and Julieke Hupkes (unpublished).
[9]P. A. Flinn (private communication).
[10]R. W. Grant, R. M. Housley, and U. Gonser, Phys. Rev. 178, 523 (1969).
[11]S. Goldsztaub, Bull. Soc. Franc. Mineral 58, 6 (1935).
[12]R. M. Housley, N. E. Erickson, and J. G. Dash, Nucl. Instr. Methods 27, 29 (1964). An additional small background correction of about 2% was made to account for Compton scattering from a Lucite source holder. This correction could be estimated only approximately which increased the uncertainty in the absolute areas but had a negligible effect on the absorption-area ratios.
[13]S. Goldsztaub, Compt. Rend. 198, 667 (1934).
[14]M. D. Lind, Acta Cryst. B26, 1058 (1970).
[15]Throughout this paper a descriptive notation is used, namely, that the "direction" of V_{zz} implies the direction of the z principal axis of the diagonalized EFG, etc.
[16]Unless stated otherwise, the quoted error represents 1 standard deviation of the mean value based on the 22 independent measurements.
[17]R. M. Housley, R. W. Grant, and U. Gonser, Phys. Rev. 178, 514 (1969).
[18]R. M. Housley, J. G. Dash, and R. H. Nussbaum, Phys. Rev. 136, A464 (1964); the effective f of our source was reduced by $\approx 1\%$ because of resonant self-absorption.
[19]A. H. Muir, Jr., K. J. Ando, and H. M. Coogan, *Mössbauer Effect Data Index* 1958-1965 (Interscience, New York, 1966).
[20]U. Gonser and R. W. Grant, Phys. Status Solidi 21, 331 (1967).
[21]C. E. Johnson, W. Marshall, and G. J. Perlow, Phys. Rev. 126, 1503 (1962).
[22]U. Gonser, R. W. Grant, H. Wiedersich, and S. Geller, Appl. Phys. Letters 9, 18 (1966).
[23]W. Rubinson and K. P. Gopinathan, Phys. Rev. 170, 969 (1968).
[24]D. P. Johnson, Phys. Rev. B 1, 3551 (1970).
[25]D. Sengupta and J. O. Artman, Phys. Rev. B 1, 2986 (1970); J. O. Artman, F. deS. Barros, J. Stampfel, J. Viccaro, and R. A. Heinz, Bull. Am. Phys. Soc. 13, 691 (1968); J. O. Artman and J. C. Murphy, Phys. Rev. 135, A1622 (1964).
[26]R. M. Sternheimer, Phys. Rev. 130, 1423 (1963).
[27]R. W. Grant, J. Appl. Phys. (to be published).
[28]R. Ingalls, Phys. Rev. 188, 1045 (1969).
[29]A. J. Nozik, and M. Kaplan, Phys. Rev. 159, 273 (1967).
[30]C. E. Johnson, Proc. Phys. Soc. (London) 92, 748 (1967).
[31]J. Chappert, R. B. Frankel, A. Misetich, and N. A. Blum, Phys. Letters 28B, 406 (1969); Phys. Rev. 179, 578 (1969).
[32]H. R. Leider and D. N. Pipkorn, Phys. Rev. 165, 494 (1968).
[33]F. S. Ham, Phys. Rev. 160, 328 (1967).
[34]R. M. Housley and U. Gonser, Phys. Rev. 171, 480 (1968).

PHYSICAL REVIEW B VOLUME 3, NUMBER 3 1 FEBRUARY 1971

Time-Reversal Experiments in Dipolar-Coupled Spin Systems*

W-K. Rhim, A. Pines, and J. S. Waugh
Department of Chemistry and Research Laboratory of Electronics, Massachusetts Institute of Technology, Cambridge, Massachusetts 02139
(Received 3 September 1970)

By applying a suitable sequence of strong rf fields, a system of dipolar-coupled nuclear spins can be made to behave as though the sign of the dipolar Hamiltonian had been reversed. The system then appears to develop backward in time, and states of nonequilibrium magnetization can be recovered in systems which would superficially appear to have decayed to equilibrium. This behavior is consistent with dynamical and thermodynamical principles, but shows that the spin-temperature hypothesis must be employed with caution. The theory of the time-reversal phenomenon is discussed, including the practical limitations on the accuracy with which it can be achieved. Various echo experiments in the laboratory and in the rotating frame are reported. The application of repeated time reversals to the problem of high-resolution NMR in solids is discussed.

I. INTRODUCTION

One's first impression on seeing a spin echo tends to be of having witnessed a spontaneous fluctuation of an apparently disordered system into an ordered (magnetized) state. Actually, of course, the system was by no means as disordered as it seemed to be: It had to be prepared from a magnetized state in a special way, such that its microscopic dynamical equations guaranteed a return to the magnetized state; and the name "echo" of course expresses just this fact. The importance of a dynamical, as opposed to thermodynamical, interpretation is particularly transparent in the case of the Hahn echo.[1-3] There the spin Hamiltonian is *inhomogeneous*, i.e., it represents a sum over uncoupled spins or isochromats interacting with fixed local fields. One is not dealing with a "many-body" system at all, and the formation of an echo is easily understood by superposing the quantum-

mechanical (or classical) motion of individually precessing magnetic moments. The same is true of quadrupole echoes,[4,5] though a purely classical picture is not quite so convenient there, and also of photon echoes,[6] whose interpretation follows the same lines as the Hahn echo if a fictitious spin[7] is suitably introduced.

One feels intuitively that the situation ought to be different in the case of *interacting* particles, such as the nuclear spins in a rigid solid. There "spin diffusion" prevents one's using pictures based on isochromats moving in local fields. Moreover, there is no known way to integrate the microscopic dynamical equations even approximately over times much longer than T_2, the time which characterizes the decay of transverse magnetization from an initially coherent state. Under these circumstances recourse is made to the "spin-temperature" hypothesis,[8-10] which asserts that the system approaches a state which is adequately described as one of internal equilibrium (sometimes called semi-equilibrium, to emphasize that the spin system can be considered isolated from the surrounding lattice only for a certain time T_1, usually much greater than T_2).

A particularly simple internal equilibrium state is obtained by first polarizing the system for a long time in a very strong external field $H_0 \gg H_{\rm loc}$, where $\gamma H_{\rm loc} \sim T_2^{-1}$. The state of the system is then assumed to belong to a canonical ensemble characterized by the lattice temperature T_l:

$$\sigma_z(0) = (1/Z)\, e^{-\mathcal{H}_z/kT_l}\,, \qquad \mathcal{H}_z = -\gamma H_0 I_z + O(\gamma H_{\rm loc})\,. \tag{1}$$

We shall henceforth speak in terms of the reduced density matrix

$$\rho_z(0) = 1 + \gamma H_0 I_z/kT_l \tag{2}$$

appropriate to the high-temperature approximation and to the removal of $Z \sim (2I+1)^N$. A 90° pulse of resonant rf field is now applied to bring the magnetization along the y direction:

$$\rho_y(0) = 1 + \gamma H_0 I_y/kT_l\,. \tag{3}$$

The magnetization $\gamma\langle I_y\rangle$ now precesses about $\vec{H}_0$ {because $[\rho_y(0), \mathcal{H}_z] \neq 0$} and decays to zero {because $[\rho_y(0), \mathcal{H}_{\rm int}] \neq 0$}, where $\mathcal{H}_{\rm int}$ is the Hamiltonian of the spin-spin interactions. If the system approaches internal equilibrium, it is then to be described by

$$\rho(\infty) = 1 - \mathcal{H}_z/kT_s\,. \tag{4}$$

Since Zeeman energy must be conserved under the time-independent Hamiltonian acting during the decay,

$$E(\infty) = E(0) = \mathrm{Tr}[\rho_y(0)\,\mathcal{H}_z] = 0\,, \tag{5}$$

one must set the spin temperature $T_s = \infty$ in (4). Thus $\rho(\infty) = 1$. It is now clear that no echo phenomena can be evoked by applying any external fields: The Hamiltonian representing their interactions with the system commutes trivially with $\rho(\infty)$.

To be sure, some echo phenomena are known in solids.[11,12] However, these echoes can be evoked only by interrupting the development of $\rho_y(0)$ *before* the system has had an opportunity to approach the postulated equilibrium state, and they are weaker the longer that decay is permitted to proceed before interruption.

In this paper, we shall describe a form of echo[13] which can be made to occur even after $\rho_y(0)$ has been allowed to develop for a time much greater than T_2. Its occurrence shows that the spin-temperature hypothesis in the simple form employed above is not correct. Of course, no violation of the second law of thermodynamics is implied, and the spin-temperature hypothesis retains its utility in describing *most* NMR experiments in solids. We shall return to this point later.

Briefly, the experiments depend on the fact that the time development of the system is dynamically reversible in a microscopic sense, whereas it may behave irreversibly on a thermodynamic scale. The apparent conflict between these manifestations is sometimes called Loschmidt's paradox.[14] We shall find it useful to introduce the concept of a "Loschmidt demon" who is able to reverse the dynamical behavior of a system, thereby retracing a path which *seemed* to be irreversible. The Loschmidt demon differs from the familiar Maxwell demon in that he accomplishes the reversal by changing the sign of the system Hamiltonian rather than by exercising control over microscopic dynamical variables. Since the state of the system obeys the Schrödinger equation

$$\psi(t) = e^{-i\mathcal{H}t}\psi(0)\,,$$

such a sign reversal is clearly equivalent to a reversal of the time coordinate.

In Sec. II, we show how this is done, and dispel any doubts about its conflict with thermodynamic principles. In Sec. III, we give the results of several experiments. The theory is expanded in Sec. IV, and Sec. V describes an important extension and application of this phenomenon.

II. SIMPLE TREATMENT

A. Theory

The spin Hamiltonian in which we will be mainly interested is the dipole-dipole coupling $\mathcal{H}_d$ in a rigid lattice of like spins $\vec{I}_i$, or, more precisely, the truncated form of this interaction $\mathcal{H}_d^0$ appropriate to the reference frame R which rotates at the spectrometer frequency ω about a very strong Zeeman field $H_0 = \omega_0/\gamma$ in the z direction. We have

$$\mathcal{H}_d^0 = \sum_{i<j}\sum b_{ij}(\vec{I}_i \cdot \vec{I}_j - 3I_{zi}I_{zj}) ,$$
$$b_{ij} = \gamma^2 \hbar r_{ij}^{-3} P_2(\cos\theta_{ij}) . \quad (6)$$

The Loschmidt demon will convert $\mathcal{H}_d^0$ into $k\mathcal{H}_d^0$, with k a negative number, so that the system retraces its previous normal dipolar development and departs from what appears to be a state of equilibrium, as mentioned in Sec. I. This conversion cannot be made in a literal sense, but its effects can be simulated through the agency of suitable external forces.[15] Suppose a strong rf field $(2\omega_1/\gamma)\cos\omega t$ is applied in the x direction with $|\omega_0 - \omega| \ll \omega_0$. The Hamiltonian in the rotating frame now includes in addition to (6), the Zeeman effect due to the field

$$[\omega_1 \vec{I} + (\omega_0 - \omega)\vec{k}]/\gamma .$$

As Redfield has shown,[16] it is convenient to view the system from the vantage point of the doubly (tilted) rotating frame (DTR), defined by the transformations

$$\rho_{\mathrm{DTR}} = \mathrm{DTR}\,\rho_{\mathrm{LAB}}(\mathrm{DTR})^{-1} ,$$
$$R = e^{-i\omega t I_z} ,$$
$$T = e^{i\xi I_y} ; \quad \tan\xi = \omega_1/(\omega_0 - \omega) , \quad (7)$$
$$D = e^{-i\omega_e t I_z} ; \quad \omega_e = [\omega_1^2 + (\omega_0 - \omega)^2]^{1/2} .$$

In this frame the density matrix obeys the Liouville equation

$$\frac{\partial}{\partial t}\rho_{\mathrm{DTR}} = -i[\mathcal{H}_{\mathrm{DTR}}, \rho_{\mathrm{DTR}}] , \quad (8)$$

with

$$\mathcal{H}_{\mathrm{DTR}} = \mathcal{H}_d^0 P_2(\cos\xi) + \mathcal{H}_{ns} , \quad (9)$$

$$\mathcal{H}_{ns} = \tfrac{3}{2}\sin\xi\cos\xi \sum_{i<j}\sum b_{ij} \times [(I_{+i}I_{zj} + I_{zi}I_{+j})\, e^{-i\omega_e t} + \mathrm{c.c.}]$$
$$- \tfrac{3}{4}\sin^2\xi \sum_{i<j}\sum b_{ij}(I_{+i}I_{+j}e^{-2i\omega_e t} + \mathrm{c.c.}) . \quad (10)$$

When ω_e is large ($\omega_e T_2 \gg 1$), the oscillatory part $\mathcal{H}_{ns}$ can be removed for purposes of calculating the secular development of the system, just as one truncates the ordinary rotating frame Hamiltonian $\mathcal{H}_R$ to obtain (6) when $\omega_0 T_2 \gg 1$. We will discuss this step more fully later. Assuming it to be valid, we see that (9) has the desired form $k\mathcal{H}_d^0$, with k adjustable between 1 and $-\frac{1}{2}$ at the experimenter's discretion.

Remember, however, that this result refers to observations made in the DTR frame, and does not by itself embody a means of reversing the time development of ρ_R in the rotating frame. In fact, the full effect on ρ_R of applying a burst of effective field ω_e/γ for a time t_B is more complicated:

$$\rho_R(t_1 + t_B) = T^{-1}D^{-1}\exp[-it_B\mathcal{H}_d^0 P_2(\cos\xi)]DT\,\rho_R(t_1)$$
$$\times T^{-1}D^{-1}\exp[it_B\mathcal{H}_d^0 P_2(\cos\xi)]DT . \quad (11)$$

It can be simplified by modifying the experiment in the following two ways:

(a) Make the duration of the burst by a resonant number of periods of the precession about $\vec{\omega}_e$: $\omega_e t_B = 2n\pi$, then $D = D^{-1}$ in (11).

(b) Immediately precede the curst by a resonant rf pulse chosen to rotate any magnetization present through an angle ξ about the y axis of the rotating frame (i.e., the rf carrier in the pulse is in phase quadrature to that in the burst), and terminate it by a similar pulse rotation through $-\xi$. The effects of these pulses can be represented by $e^{\mp i\xi I_y} = T^{\mp 1}$ acting on ρ_R which annihilate the transformations T, T^{-1} in (11).

The effect of this treatment is then simply

$$\rho_R(t_1 + t_B) = \exp[-it_B\mathcal{H}_d^0 P_2(\cos\xi)]\rho_R(t_1) \times \exp[it_B\mathcal{H}_d^0 P_2(\cos\xi)] , \quad (12)$$

and the Loschmidt demon has been realized if we choose ξ such that $P_2(\cos\xi) < 0$. Just this procedure for interconversion between reference frames has been employed by Jeener *et al.*[17] but not for the same purpose. If it is to be used for time reversal over reasonably long times it suffers from a severe practical limitation: Any appreciable inhomogeneity in the applied field, especially the rf field, will result in failure to satisfy condition (a) above in all parts of the sample. The result is a quick destruction of the coherence of the inverse time development and failure of the experiment. This difficulty can be circumvented by adding the further condition:
(c) Periodically reverse the direction of $\vec{\omega}_e$ (i.e., the rf carrier phase and the offset from resonance, $\omega_0 - \omega$). By this means the dephasing of isochromats caused by field inhomogeneity is prevented from accumulating. (There are theoretical benefits to be gained by this procedure even if the fields are homogeneous, as we will see later.) The reversal should be made as often as possible, but at integral multiples of the period expressed in (10). For the general case, a reversal could be made every $2\pi/\omega_e$ sec. For the special case of exact resonance ($\xi = \frac{1}{2}\pi$), the first term of (10) vanishes, and the reversal can be made twice as often if desired, i.e., the burst consists of a train of contiguous phase-alternated 180° pulses. From now on we restrict ourselves to the exact resonance case ($\xi = \frac{1}{2}\pi$), as this was the one adopted for the majority of our experiments.

In summary, the free dipolar time development of the spin system which occurred at a time t can be reversed by applying for a time $2t$ a special

sequence consisting of a pair of 90° pulses along the $+y$ and $-y$ axes of the rotating frame, enclosing an even number of contiguous n_π pulses which alternate between the $+x$ and $-x$ axes: Calling this sequence $B(t_B)$ we have the equivalence

$$e^{+i\mathcal{H}_d^0 t_B/2} \rightleftarrows B(t_B) \ .$$

$B(t_B)$ is depicted in Fig. 1(a). All this evidently holds for any interaction with the same transformation properties as $\mathcal{H}_d^0$. We now present a simple pictoral representation of these equations and apply it to a well-known experiment.[13]

B. Simple Picture

The normal inhomogeneous spin echo[1,2] is very conveniently described in terms of the evolution of spin isochromats which precess at different frequencies about an external inhomogeneous magnetic field. The behavior of dipolar-coupled spins, on the other hand, is normally not amenable to such a simple "hand-waving" description. However, even for these systems, the simple picture of inhomogeneously perturbed noninteracting spins is sometimes valuable, and if employed carefully, allows a simple understanding of many experiments as well as facilitating further extensions and predictions.[18,19]

We describe here the use of such a model which is appropriate for some of our experiments and

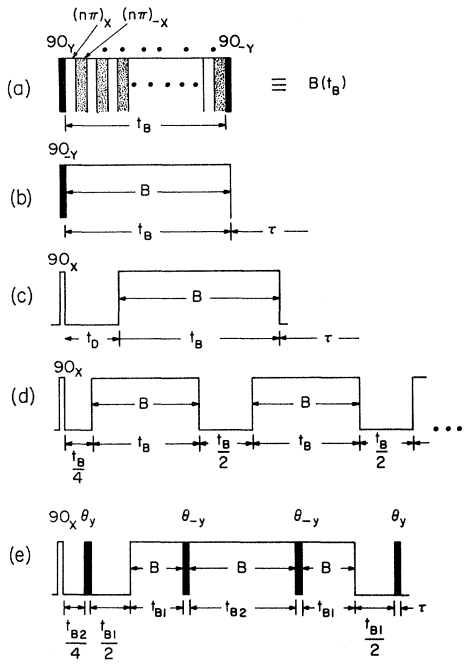

FIG. 1. Pulse sequences used for various experiments. $B(t_B)$ in (a) is the time-reversing sequence referred to in the text, and is depicted as B in the other pulse sequences. θ_μ or $(\theta)_\mu$ means a $\theta°$ pulse along the μ axis of the rotating frame.

utilizes Eqs. (7)–(9) with $\xi = 90°$ as a guideline for its construction. The discussion takes place in the reference frame rotating at frequency ω_0 about the z axis. With no rf applied we adopt the well-known picture of spin isochromats in an inhomogeneous field in the z direction. There is a distribution between fast to slow isochromats (labeled 1 and 2 in Fig. 2) which precess, respectively, clockwise and anticlockwise about the z axis. During an rf burst along the x axis we use a similar picture with the following differences: The inhomogeneous field is now along the x axis and the sense of precession of the isochromats about this axis is opposite to that about z. Further, the rate of precession is reduced by a factor of 2. 90° pulses are treated as usual, whereas the system is invariant to 180° pulses. These stipulations incorporate pictorially the main features of Eqs. (7)–(9): (i) The rf burst converts the effective Hamiltonian from $\mathcal{H}_d^0$ in the rotating frame to $-\frac{1}{2}\mathcal{H}_d^0$ in the tilted rotating frame [taking account of (iii)]. (ii) 90° y pulses transform the density matrix to and from the above frames. (iii) Our time scale during the burst is limited to integral cycle times of the rf field.

Figure 2 demonstrates the application of this simple picture to the echo experiment described previously[13] and referred to again in Sec. III. We see that most of the qualitative features of the experiment are incorporated neatly in this description, but we emphasize that this should not be taken too seriously and serves only as a useful pictorial accessory when used in conjunction with the appropriate equations. The reader will no doubt appreciate the trivial extension to multiple echoes described briefly in Secs. III and V.

C. Remarks on Statistical Mechanics

For an echo of magnitude M_0 to occur at time $t = 0$ in an isolated system of energy E_0, the representative point of the system must lie in some region $\mathcal{S}(0)$ of the phase space. This region is much smaller than the total constant-energy surface $\mathcal{E}_0$, expressing the fact that the magnetized state is one of low entropy. Every possible representative point in $\mathcal{S}(0)$ arrived there from a sequence of earlier locations, completely determined by the system Hamiltonian through the microscopic equations of motion. That is, a knowledge of $\mathcal{H}$ specifies a sequence of mappings of $\mathcal{S}(0)$ onto the precursor regions $\mathcal{S}(-t)$. The problem confronting an experimenter who wishes to produce an echo at time $t = 0$ is how to prepare a system which is known to be in $\mathcal{S}(-t_0)$.

This is a more subtle task than to prepare the system in $\mathcal{S}(0)$. The latter can be accomplished, for example, by bringing the spins to equilibrium with a lattice in a strong field and then applying a

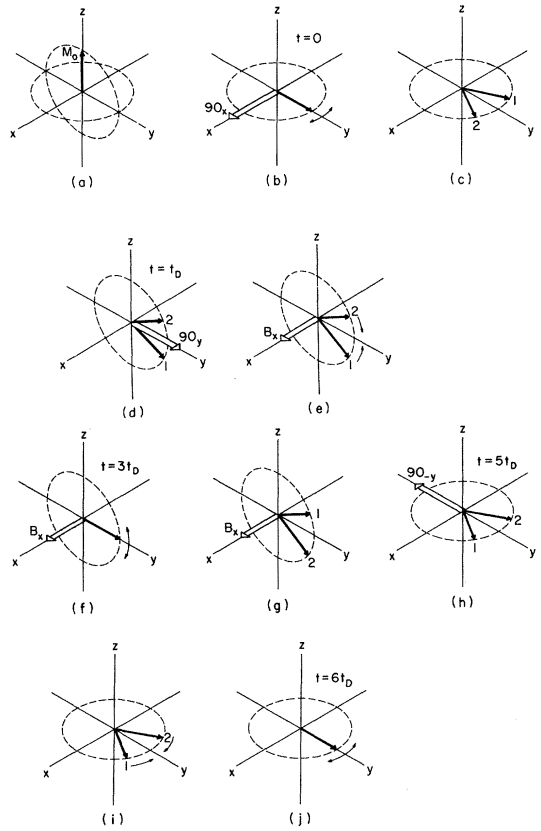

FIG. 2. Rotating-reference-frame description of the spin echo in Fig. 4, using the simple picture in Sec. II. The spin system in equilibrium (a) is irradiated at time $t=0$ with a 90° pulse along the x direction (90_x) nutating the magnetization into the x-y plane (b). The magnetization decays with "fast" spins precessing clockwise and "slow" spins anticlockwise about the z axis, and we see a normal free induction decay (c). At time $t=t_D$ a 90_y pulse brings the dephased spins into the y-z plane (d) and a rf burst is applied along the x axis. According to our picture the spins now precess about the x axis with "slow" and "fast" spins having interchanged their sense of precession (e), and refocus at time $t=3t_D$ (f). This produces the rotary echo described in Sec. III. The spins now dephase about the x axis (g) and at $t=5t_D$ the rf burst is terminated with a 90_{-y} pulse which returns the dephased spins to the x-y plane (h). We now have situation (c) except that the "fast" and "slow" spins are interchanged in position (i) and the spins rephase leading to a spontaneous echo (j) observed in Fig. 4. Note that the time-reversing rf sequence in (d) through (h) is analogous, for the case of homogeneous dipolar-coupling, to the 180° refocusing pulse employed for the normal inhomogeneous spin echo.

90° pulse: It requires only the ability to establish specified values of the macroscopic variables M and E, since $\mathcal{S}(0)$ includes by definition all dynamical states consistent with these values. $\mathcal{S}(-t_0)$, on the other hand, cannot be specified by macroscopic variables alone but requires a knowledge of *all* the dynamical variables and how they change over a time t_0 under the influence of the equations of motion. The necessary knowledge and ability of selection characterize the Maxwell demon, who violates the second law of thermodynamics in playing his role.

The Loschmidt demon needs no such microscopic control. Beginning with a system prepared in $\mathcal{S}(0)$ as described above, he changes the sign of the Hamiltonian function of the system. After a time t_0, $\mathcal{H}$ is returned to its normal form. The change is to be accomplished by external means which make no reference to the dynamical state of the system. An analogy is useful here to a gas of molecules interacting according to a potential $U(r)$:

$$\mathcal{H}=\sum_{i=1}^{N}\frac{1}{2m_i}\,\vec{p}_i\cdot\vec{p}_i+\sum\sum_{i<j}U_{ij}(r_{ij})\ .$$

A second kind of Maxwell demon exploits the apparent possibility of recalling the previous history of the gas by reversing the signs of all $\vec{p}_i$ at some instant. It might seem that such a reversal would require a knowledge of the dynamical state at that instant (although Hahn has pointed out in discussion a case of two dimensions in which it apparently does not). Note also that the sign of $\mathcal{H}$ is not changed. The Loschmidt demon, as we define him, might instead change the signs of all the m_j and U_{ij}. Such an action certainly requires no knowledge of the dynamical state. It implies a degree of control over the *nature* of the system which may be difficult to credit in the case of gas dynamics but which clearly can be exercised, as we have seen, in certain restricted spin systems. The question of the class of Hamiltonians for which a Loschmidt demon is in principle realizable is an interesting but unsolved one.

How does the spin-temperature hypothesis fit into this discussion? In its strong form it would claim that a distribution $\rho(0)$ uniformly occupying $\mathcal{S}(0)$ at the beginning of a Bloch decay would come to fill the much larger region $\mathcal{S}_0$ uniformly after several times T_2. However, Liouville's theorem tells us that the total volume of $\mathcal{S}(t)$ is conserved. The fact is that $\mathcal{S}(t)$ may come to fill $\mathcal{S}_0$ in a coarse-grained sense only. $\mathcal{S}(0)$ is relatively compact, but $\mathcal{S}(t>T_2)$ is complicated and has a large surface-to-volume ratio, as it were, especially if forces are present between the particles of the system.[14] Thus, *for many purposes* the distribution may be treated as though it filled $\mathcal{S}_0$ uniformly. However one must be on guard against performing manipulations which inadvertently exploit the dynamical history of the system to bring $\mathcal{S}(t)$ into a condition characterized by "nonequilibrium" values of the macroscopic observables. It is worth noting that some of the experiments of Jeener *et al.*,[17] which

seemed to verify the spin-temperature hypothesis, might well have done the contrary, had their experimental conditions been adjusted somewhat differently.

Finally, we remind the reader that our experiments on solids do not actually involve a reversal in sign of $\mathcal{H}$: During the rf burst the representative point *appears* to move under a Hamiltonian $-\frac{1}{2}\mathcal{H}_d^0$ from the viewpoint of a phase space which is accelerated with respect to the "ordinary" one, the net effect upon conclusion of the time-reversing sequence being to bring the system into $\mathcal{S}(-t_0)$. The language one uses to describe the motion of the system depends, as always, on the representation in which the motion is viewed.

III. EXPERIMENTS

In this section we describe some experiments based on the properties of the time-reversing sequence described in Sec. II. All experiments were performed at the exact ^{19}F resonance frequency of 54 MHz on a single crystal of CaF_2 oriented approximately along the (110) direction. The peak H_1 field was ~100 G and our pulses had rise and fall times of ~150 nsec. The apparatus is to be described in more detail elsewhere.[20]

A trivial experiment is one in which $B(t_B)$ is applied to the spin system initially in equilibrium with the lattice in a field H_0. $B(t_B)$ reverses the (nonexistent) time development of the z component of the magnetization, leaving the system in its original state.

A more interesting case is the reversal of the time development of the x, y components. Assume, therefore, that we apply the pulse sequence of Fig. 1(b) with $n = 1$, consisting of a time-reversing sequence preceded by a 90_{-y} pulse. (Note that this pulse is immediately negated by the leading 90_y pulse of the time-reversing sequence. In practice we simply omit both from the experiment.) During the burst the system undergoes a reversed dipolar development with Hamiltonian $-\frac{1}{2}\mathcal{H}_d^0$ corresponding to a normal rotary free induction decay at resonance, treated for example by Goldburg and Lee.[21] At time t_B the system reverts to normal dipolar development and should return to the initial state at $\tau = \frac{1}{2}t_B$ as indicated by the appearance of an echo. This sequence is formed by stages (f)–(j) of Fig. 2. The result of the experiment is shown in Fig. 3. The open circles depict the magnetization along the y axis during the burst and were obtained by observing the signal immediately following the receiver dead time of about 2 μsec without the final 90_{-y} pulse, while the number of $(x, -x)$ pulse pairs was varied. The oscillations were introduced deliberately for this part of the data by misadjusting the pulse widths during the burst and having x pulses of nutation angle $\pi - \alpha$ and $-x$ pulses of nutation angle $\pi + \alpha$ with $\alpha \simeq 25°$. This introduces a slow accumulative precession of frequency $\omega_1\alpha/\pi$ which leads to the observed oscillations, and the free induction decay envelope can be extracted simply by inspection as indicated in the figure. This is necessary because any slower oscillations due to small misadjustments, which are almost unavoidable, would make extraction of the envelope a much less certain proposition. The full circles show the observed echo whose maximum comes at $\frac{3}{2}t_B$, as expected. The shape of the rotary free induction decay is the same as that of the normal free induction decay except stretched by a factor of 2, as observed previously.[21–23]

In the experiment of Fig. 4 (which is the one described by the simple picture of Fig. 2), we first apply a 90_x pulse after which we see a normal free induction decay. The time-reversing sequence with $n = 1$ is then applied as in Fig. 1(c) such that $t_B = 4t_D$, and at time $\tau = t_D$ we see the expected echo. Figure 5 shows the initial decay (full circles) and also the magnetization during the burst (open circles) with the data collected as before by misadjusting the π pulse widths and omitting the final 90_{-y} pulse. The envelope shows a rotary spin echo (which is of course entirely different in character from the inhomogeneous rotary spin echo observed by Solomon[24]). The width is stretched by a factor of 2 and we see that the

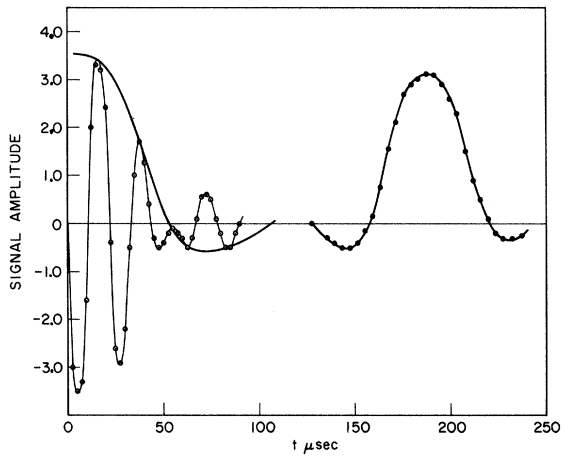

FIG. 3. Transient magnetization of ^{19}F nuclei in CaF_2 observed along the y axis of the rotating frame using the pulse sequence of Fig. 1(b). The closed circles depict the echo obtained in this experiment with a rf burst of ~120 μsec. In order to see the evolution of the magnetization during the burst the final 90_{-y} pulse was omitted and the number of pairs of $(x, -x)$ pulses was varied, leading to the data recorded as open circles. The oscillations were introduced deliberately for this part of the experiment as explained in the text, and the envelope is drawn by inspection. Note the characteristic beat structure in the rotary free induction decay.

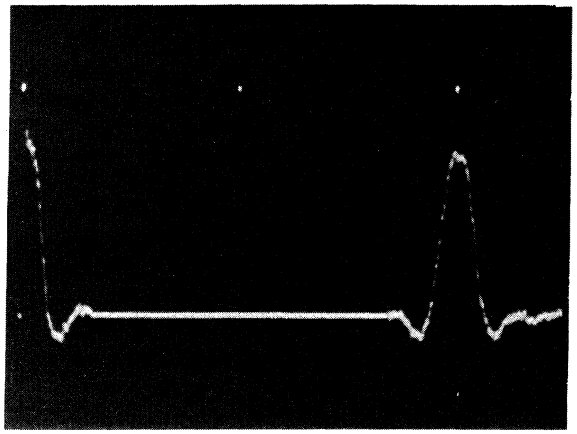

FIG. 4. Oscilloscope trace of the ^{19}F transient magnetization in CaF_2 using the pulse sequence of Fig. 1(c). Following the initial free induction decay a time-reversing burst (B) is applied at the noise-free section of the trace and an echo then appears, $t_D = 88\ \mu$sec, $t_B = 350\ \mu$sec. This is the experiment described by the simple picture of Fig. 2.

shape and beat structure are again preserved by our phase-alternation technique.

In this experiment, we have obtained substantial echoes for burst lengths of up to 650 μsec, meaning a recovery of the magnetization after about 1 msec from the first 90° pulse. The reasons for decay of the echo amplitude are discussed later and are probably dominated by machine instabilities and errors. Figure 6 demonstrates that the same effect may be obtained by using a train of narrow phase-alternated 90_x pulses in the time-reversing sequence instead of the contiguous $n\pi$ pulses, since the secular part of the Hamiltonian is the same for both. A nice feature of this experiment is the direct observation of the rotary echo during the pulse train. The efficiency of this pulse train for longer bursts, however, is lower than that of 1(a) if compared using the same average rf power. This point is brought up again in Sec. V.

$t_B = 2t_D$ corresponds to the peak of the rotary echo and Fig. 7 shows the signal observed in an experiment where the burst is terminated soon after this point without the final 90_{-y} pulse. We see a large recovery of the magnetization with $t_D = 133\ \mu$sec, which is substantially larger than T_2. (The negative signal is due to a peak negative value in the oscillation caused by a pulse width misadjustment or by change of the nutation angle due to rf power droop during the burst.)

Figure 8 shows that if we apply an additional time-reversing sequence at $\tau = 2t_D$ another echo appears, and this may of course be extended to multiple echoes in a manner analogous to that of Carr and Purcell.[25] The efficiency with which these echoes are summoned suggests that such echo trains might form the basis of a powerful approach to the problem of line narrowing in solids. This is treated briefly in Sec. V.

As a final demonstration of a simple application of the time-reversing sequence, let us look at the experiment of Fig. 9 which employs the pulse sequence in Fig. 1(e) with $\theta = 90°$. The first 90_y pulse following the free induction decay produces the well-known "solid

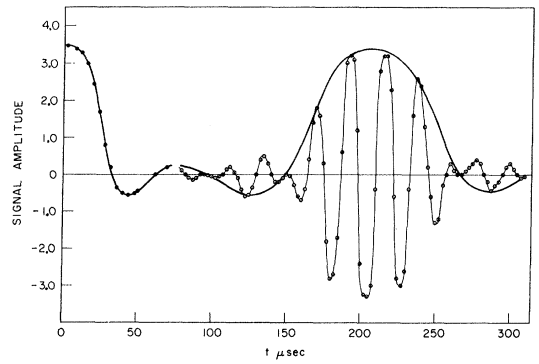

FIG. 5. Experiment designed to show the evolution of the magnetization during the rf burst in an experiment like that of Fig. 4. This is done as in Fig. 3 by omitting the final 90_{-y} pulse from the pulse train which follows the free induction decay (closed circles) and plotting the magnetization immediately following the burst vs burst length (open circles). The oscillations were again introduced deliberately as explained in the text. The envelope shows the "rotary echo" and note again the intact beat structure characteristic of the ^{19}F signal in CaF_2.

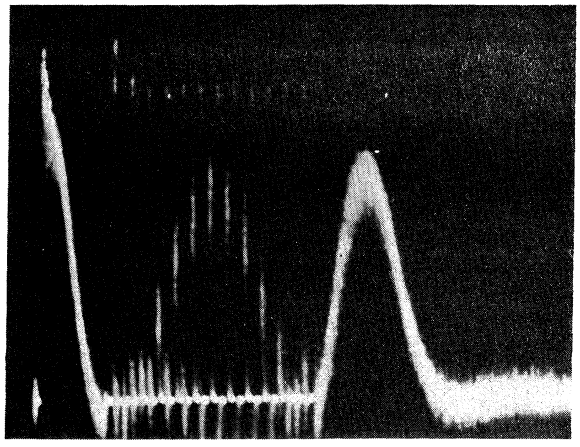

FIG. 6. Pulsed version of the experiment in Figs. 4 and 5. In this experiment, the time-reversing sequence (B) in pulse sequence 1(c) was modified by replacing the contiguous $(n\pi)_x$ and $(n\pi)_{-x}$ pulses with a train of alternate 90_x and 90_{-x} pulses spaced 5 μsec apart. In addition to the free induction decay and echo, observed as in Fig. 4, we see the "rotary echo" of Fig. 5 during the "windows" in the pulse train.

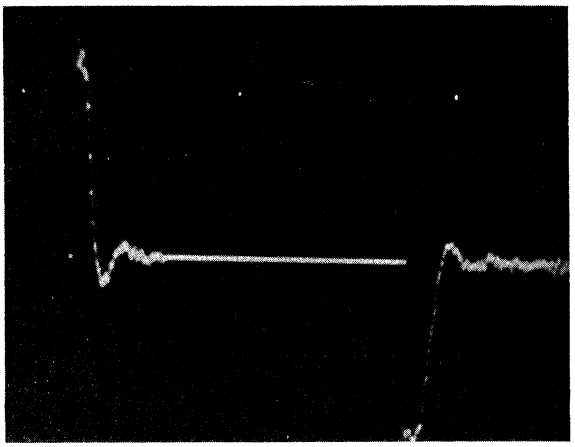

FIG. 7. Oscilloscope trace of magnetization in an experiment like that of Fig. 4. In this case, the time-reversing sequence terminated near the peak of the rotary echo of Fig. 5 and we see a normal free induction decay. The parameters are $t_D = 133$ μsec, $t_B = 345$ μsec. The fact that the second signal has a negative value is explained in the text.

echo."[11] By sequentially using the properties of the time-reversing sequence we see that the first half of the burst brings the system back to its initial state, and the second half produces a rotary free induction decay and corresponding "rotary solid echo." Thus on terminating the burst we see a negative time development solid echo and the final 90° pulse brings the system back again to the initial state. In this way the effects of any number of pulses may be reversed. This experiment vividly demonstrates the more efficient nature of our echoes as compared to the solid echoes. This matter is referred to again in Secs. IV and V. For $\theta = 45°$, we obtain an analogous reversal of Jeener and Broeckaert's pulse sequence[19] showing that their postulated dipolar state is not an adequate description of the system for this type of experiment.

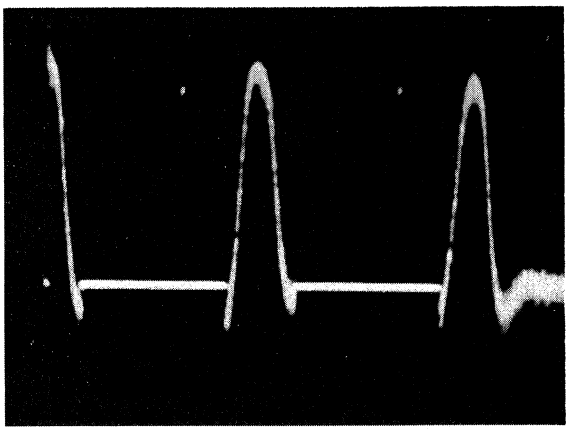

FIG. 8. Double-echo version of the experiment in Fig. 4 using pulse sequence 1(d) with $t_B = 180$ μsec. This shows that an extension of our echoes analogous to that of Carr and Purcell is possible.

IV. NONIDEALITIES

A. General Framework

The ideal treatment in Sec. II was based on the assumption that the effect of a time-reversing sequence could be represented by replacing $\mathcal{H}_d^0$ with $-\frac{1}{2}\mathcal{H}_d^0$ as the effective Hamiltonian during the burst (for the case $\xi = \frac{1}{2}\pi$). Here we investigate the validity of this assumption and discuss the effect and extent of various nonidealities encountered in practice.

We begin by writing the time development during the burst as

$$\rho_R(t_B) = U_B(t_B)\,\rho_R(0)\,U_B^\dagger(t_B)\,, \qquad (13)$$
$$U_B(t_B) = \exp[-it_B(-\tfrac{1}{2}\mathcal{H}_d^0 + \lambda V)]\,,$$

where V is some correction to $\mathcal{H}_{DTR}$ whose matrix elements are of order T_2^{-1}, and λ is a small parameter. No generality is lost at this stage by insisting that V be time independent; it may depend parametrically on t_B but in most cases to be discussed it will not have even that indirect time dependence. The nature and origin of λV will be discussed later; at present we simply investigate the consequences of (13).

It is easily shown that[26]

$$U_B(t_B) = e^{i\mathcal{H}_1^0 t_B/2}\; T\exp[-i\lambda\textstyle\int_0^{t_B} V(t)\,dt]\,, \qquad (14)$$

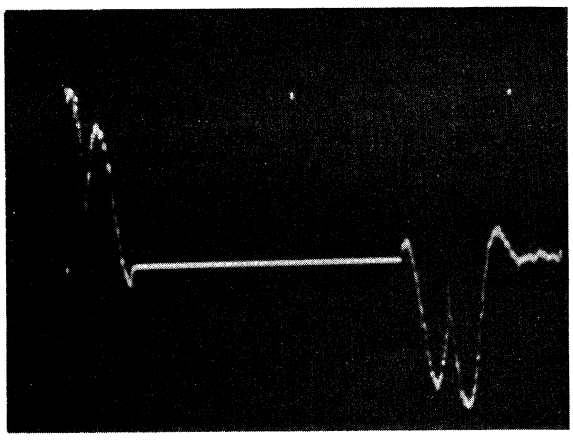

FIG. 9. Time reversal of a two-pulse experiment, using the pulse sequence in Fig. 1(e) with $\theta = 90°$. The first two pulses bring about a free induction decay and "solid echo." The following rf burst reverses this total sequence and then propagates it further backwards in time leading to the ensuing "mirror image" of the "solid-echo" experiment when the burst is terminated. The negative value of the "mirror image" is explained in the text. For this experiment $2t_{B1} + t_{B2} = 342$ μsec, corresponding to the noise-free portion of the trace.

where T is a time-ordering operator and

$$V(t) = e^{-i\mathcal{H}_d^0 t/2}\, V\, e^{i\mathcal{H}_d^0 t/2} \,. \tag{15}$$

For the condition

$$\lambda t_B \ll T_2 \tag{16}$$

we may expand the exponential in (14) to first order:

$$U_B(t_B) \approx e^{i\mathcal{H}_d^0 t_B/2} \exp[-i\lambda \textstyle\int_0^{t_B} V(t)\,dt] \,. \tag{17}$$

Now we consider the general situation in which the burst is preceded and followed by unperturbed dipolar developments of duration t_1 and t_2. The total propagator is

$$U(t_1+t_2+t_B) = e^{-it_2\mathcal{H}_d^0} U_B(t_B)\, e^{-it_1\mathcal{H}_d^0} \,. \tag{18}$$

Combining this with (17) and rearranging a little we find

$$U(t_1+t_2+t_B) = U(\tfrac{3}{2}t_B+\tau) = e^{-i\tau\mathcal{H}_d^0} e^{-i\lambda t_B \bar{V}} \,, \tag{19}$$

where $\tau = t_1 + t_2 - \frac{1}{2}t_B$ and $\bar{V}$ is given by

$$\bar{V} = (1/t_B) \textstyle\int_{-2t_1}^{t_B-2t_1} V(t)\,dt \,. \tag{20}$$

If the initial magnetization of the system was along the μ axis in the rotating frame, $\langle I_\mu(0)\rangle$, then its final value is

$$\langle I_\mu(\tfrac{3}{2}t_B+\tau)\rangle = \mathrm{Tr}(e^{-i\tau\mathcal{H}_d^0} e^{-i\lambda t_B\bar{V}} I_\mu e^{i\lambda t_B\bar{V}} e^{i\tau\mathcal{H}_d^0} I_\mu). \tag{21}$$

We now introduce the notation

$$\{|a^n\cdot b^m|\} = \mathrm{Tr}([a[a\ldots[a,I_\mu]]\ldots][b[b\ldots[b,I_\mu]]\ldots]), \tag{22}$$

where a and b appear n and m times, and

$$\{|a^n\cdot 1|\} = \{|1\cdot a^n|\} = \{|a^n|\} \,, \tag{23}$$

where the last is the bracket introduced by Waugh and Wang.[27] Using this and expanding (21) in τ and λt_B we obtain

$$\langle I_\mu(\tfrac{3}{2}t_B+\tau)\rangle = \sum_{n=0}^{\infty} M_n \frac{\tau^n}{n!} \,, \tag{24}$$

where M_n are the moments of the echo, given by

$$M_n = \sum_{k=0}^{\infty} i^{n-k} \frac{(\lambda t_B)^k}{k!} \{|\mathcal{H}_d^{0n}\cdot\bar{V}^k|\} \,. \tag{25}$$

B. Lifetime of Echo

The time $\tau = 0$ corresponds to the expected position of the echo maximum from the discussion in Sec. II. Substituting $\tau = 0$ in (24) and (25) we obtain

$$\langle I_\mu(\tfrac{3}{2}t_B)\rangle = \sum_{k=0}^{\infty} (-1)^k \frac{(\lambda t_B)^{2k}}{(2k)!} \{|\bar{V}^{2k}|\} \,, \tag{26}$$

the odd powers all vanishing, as is well known.[28]

Assuming now that $\|\bar{V}\| \sim T_2^{-1}$ and remembering condition (16) we see that (26) expresses a recovery of the magnetization with an attenuation of order $\frac{1}{2}(\lambda t_B/T_2)^2$. Thus we expect the magnetization to recover to an appreciable extent for burst lengths that satisfy condition (16) for fixed T_2 and λ. In order to estimate this, we now inquire into the sources and nature of V and the size of λ. The first place it occurs to us to look is at the truncation of $\mathcal{H}_{\mathrm{DTR}}$ carried out in Sec. II. Since $\mathcal{H}_{\mathrm{DTR}}$ of (9) is periodic and the burst contains an integral number of cycles, its effects can be replaced by those of an average Hamiltonian[29]

$$\bar{\mathcal{H}}_{\mathrm{DTR}} = \sum_{n=0}^{\infty} \bar{\mathcal{H}}_{\mathrm{DTR}}^{(n)} \tag{27}$$

whose terms are defined by a Magnus expansion over a single cycle of $\mathcal{H}_{ns}(t)$. For Eq. (10) we have the cycle time $t_c = 2\pi/\omega_e$, and thus

$$\bar{\mathcal{H}}_{\mathrm{DTR}}^{(0)} = -\tfrac{1}{2}\mathcal{H}_d^0 \,. \tag{28}$$

Cutting off (27) at this point corresponds to the well-known procedure of "truncation." The next term does not vanish: At this point remember we have not used quite the Hamiltonian of Eq. (9) since we have periodically reversed the direction of H_1. Under these conditions it is easily verified that

$$\bar{\mathcal{H}}_{\mathrm{DTR}}^{(1)} = 0 \,, \tag{29}$$

thus leaving $\bar{\mathcal{H}}_{\mathrm{DTR}}^{(2)}$ as the leading correction term. An estimate of this factor shows that it is of the order of $\frac{1}{6}(t_c/2\pi T_2)^2$ smaller than $\mathcal{H}_d^0$. Thus for this case we identify λV with $\mathcal{H}_{ns}^{(2)}$ and λ is of order $\frac{1}{6}(t_c/2\pi T_2)^2$, which for our experimental condition is about 10^{-4}. Condition (16) is thus satisfied for t_B of many msec, and taking only the nonsecular terms into account we might expect the echo to live this long. In fact, we have obtained in the echo experiment of Sec. III a more than 98% recovery of the magnetization for t_B up to 350 μsec and a 75% recovery for t_B of 500 μsec. So some other mechanism could be contributing to the destruction of the echo.

We now turn to some other errors which stem from practical sources. The treatment up till now has assumed that the time-reversing sequence contains a series of continguous ideal $(n\pi)_x$ and $(n\pi)_{-x}$ pulses. Evidently, this cannot be realized in practice because of the finite rise and fall times of the pulses which lead to "windows" in the continuous rf irradiation, since the carrier phase of the two pulses differs by π. Thus the time-reversing sequence is better represented in practice by the pulse sequence in Fig. 10.

Another source of error is the fact that the pulses may not be exactly of nutation angle $n\pi$, as this is exceedingly difficult to adjust. Accordingly, in Fig. 10 we have indicated this by writing the angles as $n\pi+\epsilon$ and $n\pi+\epsilon'$, where ϵ and ϵ' are small error angles. We assume $|\epsilon-\epsilon'| \ll |\epsilon|$ for reasons that will become clear later. We find on calculating the average Hamiltonian $\bar{\mathcal{H}}_{\mathrm{DTR}}^{(0)}$ in this case and taking only the first order in ϵ and δ, where $1-\delta$

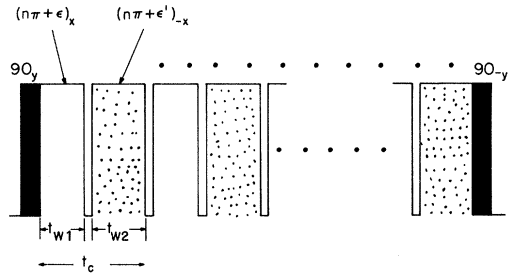

FIG. 10. Nonideal time-reversing sequence discussed in Sec. IV.

$= (t_{w_1} + t_{w_2})/t_c$:

$$\bar{\mathcal{H}}^{(0)}_{\mathrm{DTR}} = -\tfrac{1}{2}\mathcal{H}^0_d + \tfrac{3}{2}\left(\delta + \frac{\epsilon}{n\pi}\right)\sum_{i<j}\sum b_{ij}(I_{xi}I_{xj} - I_{yi}I_{yj}). \tag{30}$$

We see that $\bar{\mathcal{H}}^{(0)}_{\mathrm{DTR}}$ is of the form $-\frac{1}{2}\mathcal{H}^0_d + \lambda V$, where $\lambda \sim \delta + \epsilon/n\pi$ and $\|V\| \sim \|\mathcal{H}^0_d\|$. For $n = 1$ we have with our apparatus $\delta \sim 0.1$. With $\epsilon \simeq 0$ this would lead to very short lived echoes since $\lambda \sim \delta$. However, we see from (30) that by advertently adjusting the pulse widths away from $n\pi$ such that $\delta + \epsilon/n\pi \sim 0$, this factor can be eliminated to a certain extent. The adjustment is quite critical and requires $\epsilon < 0$ as we have indeed observed. A factor limiting this adjustment is the H_1 inhomogeneity which normally amounts to several percent. Practically, this means that ϵ is not constant over the sample and thus the adjustment $\delta + \epsilon/n\pi \sim 0$ cannot be made simultaneously over the whole sample. The H_1 inhomogeneity probably makes a significant contribution to the destruction of the echo for long bursts.

The effect of ϵ and δ becomes less serious as n is made larger since $\epsilon/n\pi$ and δ both decrease, but for large n this may be offset by a harmful increase in phase-switching cycle time.

Other machine errors not treated explicitly here probably make some additional contribution to the destruction of the echo. These include misadjustment of phases, power droop in the pulse transmitter, phase transients,[20] etc.

C. Shape of Echo

We now return to Eq. (24) and investigate $\langle I_\mu(\frac{3}{2}t_B + \tau)\rangle$ for $\tau \neq 0$, the shape of the echo about its expected maximum. An examination of (25) shows that the first term in the expansion is just the corresponding normal FID moment. The higher terms make a small contribution if condition (16) is fulfilled and lead only to a slight distortion of the echo line shape as compared to the free induction decay. This suggests a useful new means for obtaining moments of the free induction decay when the initial transient is obscured by receiver dead time; we simply produce an echo with λ small enough so that (16) is fulfilled to the desired accuracy with some particular dead time t_d [we need $t_B > 2t_d$ for pulse sequence 1(b), and $t_B > 4t_d$ for 1(c)]. This method has one important advantage over solid echoes.[11,12] In the latter, assuming a dead time t_d, the terms contributing to the distortion of the echo line shape have some inherent fixed value dependent on powers of t_d. In our case, we have the same distortion in powers of λt_B, not t_B, and this can be made arbitrarily small at least for the t_d of practical interest. Using pulse sequence 1(b) we have measured some echo line shapes for different burst lengths. These are compared with the free induction decay in Fig. 11 with no adjustable parameters except for normalization of the echo with $t_B = 110$ μsec. The agreement is very good within experimental error. For $t_B = 110$ μsec, the onset of some distortion is clearly visible. Comparison with the first part of the free induction decay is of course not possible, but the theory and other experimental evidence indicate no reason why this should not be good too. For $t_d < 10$ μsec, we need $t_B \simeq 20$ μsec and this should give us a very accurate representation of the line shape even for moderate H_1 fields. In any case, the reduction in peak echo amplitude is an indication of the amount of distortion to expect (notwithstanding the remarks below) as we have indeed found in practice.

An interesting feature of Eqs. (24) and (25) as we have seen, is the fact that the first correction term to the peak echo amplitude is in $(\lambda t_B)^2$, whereas those to the higher moments are in (λt_B). This means that distortion of the line shape should occur more rapidly than destruction of the peak echo amplitude might indicate. This is indeed evident in our experiments where for large t_B the echoes acquire a

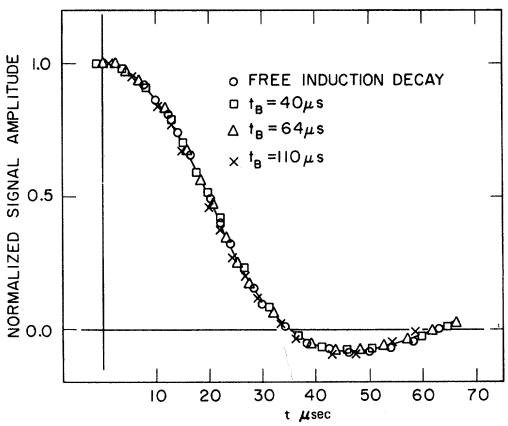

FIG. 11. Comparison of the echo line shapes of the experiment in Fig. 3 for various burst lengths. Only the right-hand portion of each echo is depicted, except for burst length 0 (free induction decay) where part of the signal is obscured by receiver dead time. No parameters are involved except the normalization of data for $t_B = 110$ μsec, where the peak echo amplitude had decreased.

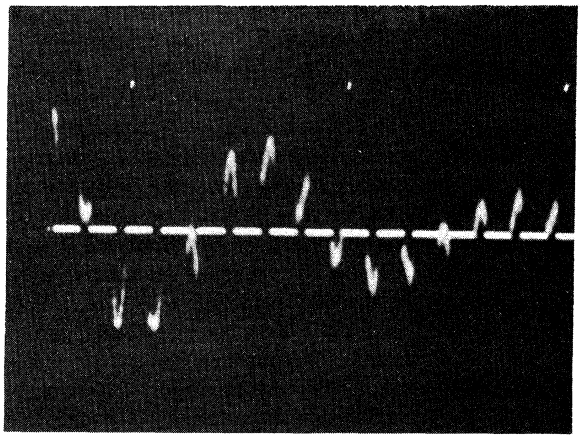

FIG. 12. Multiple-burst line-narrowing sequence [Fig. 1(d)] applied to the ^{19}F nuclei of CaF_2 with the magnet set slightly off-resonance. The cycle time $\frac{3}{2}t_B$ for this experiment was 136 μsec, and we observe a prolonged decay with a scaled off-resonance beat. This multiple-echo phenomenon has also been used to observe chemical shifts in solids in an analogous way.

progressively narrow shape corresponding to a larger destruction of magnetization for $\tau \neq 0$ than for the echo peak.

V. APPLICATION TO LINE NARROWING

A. Multiple Bursts

We have discussed at length elsewhere[29] the possibility of removing the effects of dipolar broadening by repeated application of a suitably chosen cycle of rf perturbations. These cycles have the property that the effective dipolar Hamiltonian in some suitable reference frame, while large, varies during the cycle in such a way that its net effect over a full cycle vanishes to some approximation. The present echo experiments clearly have the same property over a cycle of duration $\frac{3}{2}t_B$: The system behaves as though $\bar{\mathcal{H}}_R = \mathcal{H}_d^0$ except during the bursts where $\bar{\mathcal{H}}_R = -\frac{1}{2}\mathcal{H}_d^0$ to first order. Thus for a cycle of duration $\frac{3}{2}t_B$ the effective dipolar Hamiltonian is 0 and if the cycle is repeated indefinitely as in Fig. 1(e), the envelope of the magnetization sampled at integral cycle times should generate a very long decay corresponding to an effective line narrowing.

Consider the more interesting case in which the Hamiltonian contains chemical shifts in addition to the dipolar interaction and is given by (31). Removal of the large dipolar broadening is then a necessity if we wish to observe the fine structure associated with the chemical shifts. We have

$$\mathcal{H}_R = \mathcal{H}_d^0 + \mathcal{H}_c \ . \tag{31}$$

During the burst the effective Hamiltonian is given by

$$\bar{\mathcal{H}}_R^{(B)} = -\tfrac{1}{2}\mathcal{H}_d^0 + \bar{\mathcal{H}}_c^{(B)} + \lambda V \ ,$$

where superscript B denotes the presence of the burst and λV is a correction to the average Hamiltonian. It is easily verified that the total first correction term vanishes, including the dipolar-chemical-shift cross term, so that λV can be associated with the second correction term and λ is of order $\frac{1}{6}(t_c/2\pi T_2)^2$.

The average Hamiltonian for the total $\frac{3}{2}t_B$ cycle is

$$\bar{\mathcal{H}}_R^{(0)} = \tfrac{1}{3}(\mathcal{H}_c + 2\bar{\mathcal{H}}_c^{(B)}) + \tfrac{2}{3}\lambda V \ . \tag{32}$$

The higher correction terms depend on the symmetry of the circle. For the symmetric cycle in the pulse sequence of Fig. 1(e), we find for the total first correction term

$$\bar{\mathcal{H}}_R^{(1)} = 0, \tag{33}$$

again including the dipolar-chemical-shift cross term. The higher-order pure-dipolar correction terms evidently vanish and thus all correction terms are attenuated at least by λ or Δ, where the latter is the magnitude of the largest chemical shift. The only nonvanishing second-order term, for example, is found to be attenuated by $\sim\lambda\Delta$ from the magnitude of the usual corresponding pure-dipolar term. The normal requirement of our previous pulse experiments, namely, that we have the cycle time $t_c \lesssim T_2$, is therefore not so stringent in this experiment, and much larger cycle times should be tolerable if λ and Δ are small, as we have indeed observed. This is a good example of the exploitation of the properties of subcycles (in this case during the burst) in an effort to increase the efficiency of the full cycle.[29]

Figure 12 shows a preliminary example of the application of this pulse sequence to the ^{19}F nuclei of CaF_2 with a cycle time of 136 μsec and using 360° x and $-x$ pulses ($n = 2$). A prolonged decay with an off-resonance beat scaled by $\frac{1}{3}$ ($\bar{\mathcal{H}}_c^{(B)} = 0$), is observed: With this cycle time our previous pulse experiments fail completely.

To summarize, we mention briefly several apparent advantages of this new method as compared to some previous line-narrowing techniques. The experiment is essentially continuous wave, except for the 90_y pulses, with the magnetization sampling windows forming part of the sequence. We therefore require less power[29] than in our pulsed experiments and do not have to contend to such an extent with the adverse effects of finite pulse width. Further, the experiment does not require the additional video pulses necessary in "magic angle" experiments.[23,29] An additional advantage is the vanishing of the first-order cross correction term between dipolar and chemical-shift interactions, and the attenuation in magnitude of the higher-order correction terms. Most important we see that while t_B may be of order T_2 or more, the line-narrowing

efficiency is determined from (32) essentially by the subcycle time inside the burst, which can be made extremely small since no observation of the magnetization is necessary during this time.

Last, we mention that an analogous experiment employing only 90° rf pulses can be done if the $n\pi$ pulses in the time-reversing sequence are replaced by a train of 90° pulses along the $\pm x$ directions, but that this would not benefit from all the advantages mentioned above.

B. Symmetric Cycles

We recall from above that the total first-order correction term, including the dipolar-chemical-shift cross term, vanished both for the multiple-burst full cycle and the burst subcycle. This is a special case of a more general principle which applies to any symmetric cycle. Adopting the notation in Eq. (15) of Ref. 29, a symmetric cycle is one for which

$$\tilde{\mathcal{H}}(t) = \tilde{\mathcal{H}}(t_c - t), \tag{34}$$

where t_c is the pertinent cycle time. It is easily shown for such cycles that the first-order correction term vanishes,

$$\bar{\mathcal{H}}^{(1)} = 0. \tag{35}$$

We see that our cycle and subcycle do indeed have the requisite symmetry, leading to (35). Using (34), other sequences with this property will doubtless occur to the reader, and a general approach to elimination of the first correction term is simply symmetrization of the cycle within the constraints imposed by the requirements of the average Hamiltonian itself. A trivial example is our 4-pulse sequence.[30] Preparing the system with a 90° pulse along the y axis, it is

$$P_y - (\tau - P_x - \tau - P_{-y} - 2\tau - P_y - \tau - P_{-x} - \tau)_n .$$

It is easily verified that (34) holds over a cycle with $t_c = 6\tau$, and thus (35) is fulfilled. This sequence is simpler than a 6-pulse modification recently proposed by Mansfield,[31]

$$P_y - (\tau - P_{-x}P_y - \tau - P_{-y} - 2\tau - P_y - \tau - P_{-y}P_x - \tau)_n ,$$

and a 3-dimensional sequence proposed by Silberszyc.[32]

ACKNOWLEDGMENTS

Special thanks are due Dr. M. Mehring who constructed the rf transmitter used in these experiments and from whose advice and assistance we benefited greatly. We also acknowledge the assistance of M. G. Gibby who constructed a major part of the pulse spectrometer, the technical aid of S. Kaplan and J. D. Read, and some stimulating discussions with J. D. Ellett, Jr., R. G. Griffin, and J. M. Deutch. We thank Professor E. L. Hahn for illuminating discussions of Loschmidt's paradox.

*Work supported by the National Science Foundation and the National Institutes of Health.

[1]E. L. Hahn, Phys. Rev. 80, 580 (1950).

[2]H. Y. Carr and E. M. Purcell, Phys. Rev. 88, 415 (1952).

[3]S. R. Hartmann and E. L. Hahn, Phys. Rev. 128, 2042 (1962).

[4]I. Solomon, Phys. Rev. 110, 61 (1958).

[5]M. Bloom, E. L. Hahn, and B. Herzog, Phys. Rev. 97, 1699 (1955).

[6]I. D. Abella, N. A. Kurnit, and S. R. Hartmann, Phys. Rev. 141, 391 (1966).

[7]R. P. Feynman, F. L. Vernon, Jr., and R. W. Hellwarth, J. Appl. Phys. 28, 49 (1957).

[8]J. Jeener, *Advances in Magnetic Resonance* (Academic, New York, 1968), Vol III.

[9]M. Goldman, *Spin Temperature and Nuclear Magnetic Resonance in Solids* (Oxford U. P., London, England, 1970).

[10]A. G. Redfield, Science 164, 1015 (1969).

[11]J. G. Powles and P. Mansfield, Phys. Letters 2, 58 (1962); J. G. Powles and J. H. Strange, Proc. Phys. Soc. (London) 82, 6 (1963).

[12]E. D. Ostroff and J. S. Waugh, Phys. Rev. Letters 16, 1097 (1966).

[13]W-K. Rhim, A. Pines, and J. S. Waugh, Phys. Rev. Letters 25, 218 (1970).

[14]R. C. Tolman, *The Principles of Statistical Mechanics* (Clarendon, London, England, 1962), p. 152 ff.; G. E. Uhlenbeck and G. W. Ford, *Lectures on Statistical Mechanics* (Am. Math. Soc., Providence, R. I., 1963), Chap. 1.

[15]W-K. Rhim, Ph.D. thesis, University of North Carolina, 1969 (unpublished); H. Schneider and H. Schmiedel, Phys. Letters 30A, 298 (1969); W-K. Rhim and H. Kessemeier (unpublished).

[16]A. G. Redfield, Phys. Rev. 98, 1787 (1955).

[17]J. Jeener, R. DuBois, and P. Broekaert, Phys. Rev. 139, A1959 (1965).

[18]A. G. Anderson and S. R. Hartmann, Phys. Rev. 128, 2023 (1962).

[19]J. Jeener and P. Broekaert, Phys. Rev. 157, 232 (1967).

[20]J. D. Ellett *et al.*, *Advances in Magnetic Resonance* (Academic, New York, 1971), Vol. V.

[21]W. I. Goldburg and M. Lee, Phys. Rev. Letters 11, 255 (1963).

[22]D. Barnaal and I. J. Lowe, Phys. Rev. Letters 11, 258 (1963).

[23]M. Lee and W. I. Goldburg, Phys. Rev. 140, A1261 (1965).

[24]I. Solomon, Phys. Rev. Letters 2, 301 (1959).

[25]H. Y. Carr and E. M. Purcell, Phys. Rev. 94, 630 (1954).

[26]R. M. Wilcox, J. Math. Phys. 8, 962 (1967).

[27]J. S. Waugh and C. H. Wang, Phys. Rev. 162, 209 (1967).

[28]A. Abragam, *The Principles of Nuclear Magnetism* (Clarendon, London, England, 1961), p. 110 ff.

[29]U. Haeberlen and J. S. Waugh, Phys. Rev. 175, 453 (1968).

[30]J. S. Waugh, L. M. Huber, and U. Haeberlen, Phys.

Rev. Letters 20, 180 (1968).
[31]P. Mansfield, Phys. Letters 32A, 485 (1970).
[32]W. Silberszyc (unpublished).

PHYSICAL REVIEW B VOLUME 3, NUMBER 3 1 FEBRUARY 1971

Vacancy-Mn^{2+} Pair Spectra in Alkali Chlorides

Curt Hofer and R. R. Sharma
Department of Physics, University of Illinois, Chicago, Illinois 60680
(Received 27 April 1970; revised manuscript received 23 October 1970)

An attempt has been made to understand the fine-structure constants of the vacancy-associated-Mn^{2+} complexes corresponding to spectra III_1 and III_2 observed by Watkins in NaCl and KCl. The point-charge contributions arising from the mechanisms which were not considered previously are included in our treatment. The role of overlap and/or covalency effects are analyzed by calculations. Assuming the lattice distortions in accordance with the available calculations, the theoretical values of the fine-structure constants are compared with the experimental values. For spectra III_1 and III_2 the D and E values are smaller than the experimental values but they agree in sign if one considers point-charge and overlap effects. The inclusion of covalency effects brings, in general, the calculated values into better agreement with experiment. Some conclusions have also been drawn regarding the distortion of the lattice in order to improve the calculated values.

I. INTRODUCTION

Many theoretical and experimental attempts have been made in alkali halides to understand the interactions between a divalent ion impurity and a vacancy. The vacancy has been found to pair off with the divalent impurity to form vacancy-impurity pair complexes. It has been established by Watkin's electron paramagnetic resonance spectra[1] of Mn^{2+}-doped alkali chlorides that two different kinds of pair complexes can exist in such systems. One complex is formed when the vacancy is located at the cation site nearest to the magnetic ion, the spectra corresponding to which is designated by III_1. The other complex is formed when the bound vacancy is at the next-nearest cation site relative to Mn^{2+} impurity producing spectra III_2. These spectra have been interpreted by Watkins by means of the theory then available which considered the contributions from the spin-spin mechanism arising from $d \rightarrow s$ excitation only and the Watanabe mechanism. The theory was found to give the correct sign but the results were an order of magnitude too low. No attempt has yet been made in such systems to estimate the contributions from overlap and/or charge transfer effects, though the importance of these has been emphasized by Watkins. Since now other mechanisms are known to give dominant contributions, it is of interest to know whether the conclusions of Watkins change if one incorporates the effects of these mechanisms. This has been done in the present paper. Moreover, the contributions from overlap effects have also been calculated. The spectra we have considered in the present paper are III_1 and III_2 in NaCl and KCl crystals.

In Sec. II we present the procedure and the calculations for the ground-state splittings of the complexes III_1 and III_2 in NaCl and KCl and compare them with the experimental results. The discussion is given in Sec. III, where some speculations have also been made to bring the theoretical results into line with experiment.

II. PROCEDURE AND RESULTS

The expressions derived in Refs. 2 and 3 may be used here directly with appropriate changes to estimate the ground-state splitting parameters D and E for spectra III_1 and III_2. In the following, we first consider spectra III_1 and obtain point-charge contributions from various mechanisms[2] — Blume-Orbach (BO), spin-spin (SS) ($d \rightarrow s$, $d \rightarrow d$, $d \rightarrow g$), Watanabe-with-cubic field (WC), and Orbach-Das-Sharma (ODS) mechanisms — and overlap contributions in NaCl and KCl. Next we consider spectra III_2 and give similar results.

A. Spectra III_1

The vacancy-Mn^{2+} pair complex which gives rise to the spectra III_1 is shown in Fig. 1. Bassini and Fumi[4] have estimated the displacements of the ions for this complex in NaCl and KCl with the impurity ions Cd^{2+}, Ca^{2+}, and Sr^{2+}. To the knowledge of the authors, no similar calculations have yet been reported for the case where the impurity ion is Mn^{2+}. In the absence of such data, we assume that the displacements of the ions when Mn^{2+} is present as

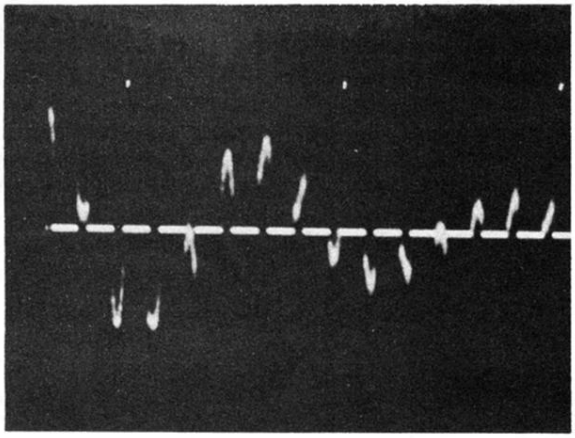

FIG. 12. Multiple-burst line-narrowing sequence [Fig. 1(d)] applied to the ^{19}F nuclei of CaF_2 with the magnet set slightly off-resonance. The cycle time $\frac{3}{2}t_B$ for this experiment was 136 μsec, and we observe a prolonged decay with a scaled off-resonance beat. This multiple-echo phenomenon has also been used to observe chemical shifts in solids in an analogous way.

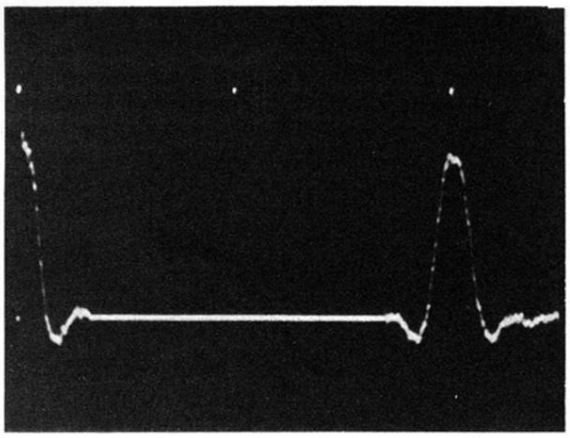

FIG. 4. Oscilloscope trace of the ^{19}F transient magnetization in CaF_2 using the pulse sequence of Fig. 1(c). Following the initial free induction decay a time-reversing burst (B) is applied at the noise-free section of the trace and an echo then appears, $t_D = 88\ \mu sec$, $t_B = 350\ \mu sec$. This is the experiment described by the simple picture of Fig. 2.

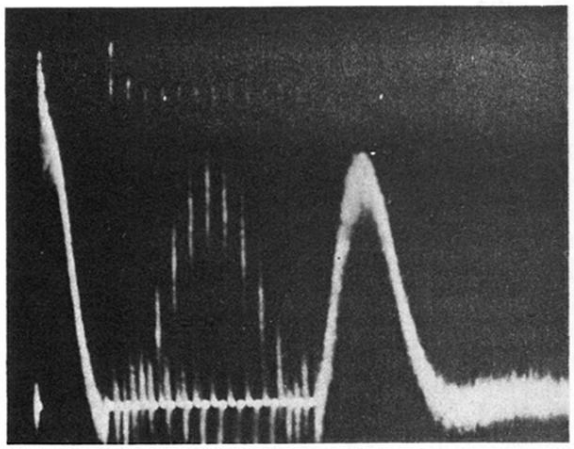

FIG. 6. Pulsed version of the experiment in Figs. 4 and 5. In this experiment, the time-reversing sequence (B) in pulse sequence 1(c) was modified by replacing the contiguous $(n\pi)_x$ and $(n\pi)_{-x}$ pulses with a train of alternate 90_x and 90_{-x} pulses spaced 5 μsec apart. In addition to the free induction decay and echo, observed as in Fig. 4, we see the "rotary echo" of Fig. 5 during the "windows" in the pulse train.

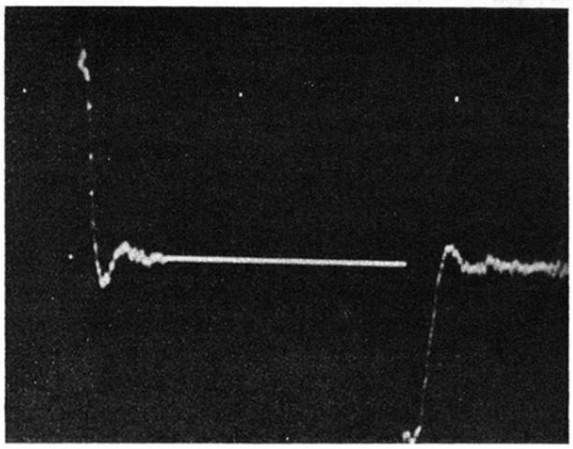

FIG. 7. Oscilloscope trace of magnetization in an experiment like that of Fig. 4. In this case, the time-reversing sequence terminated near the peak of the rotary echo of Fig. 5 and we see a normal free induction decay. The parameters are $t_D = 133$ μsec, $t_B = 345$ μsec. The fact that the second signal has a negative value is explained in the text.

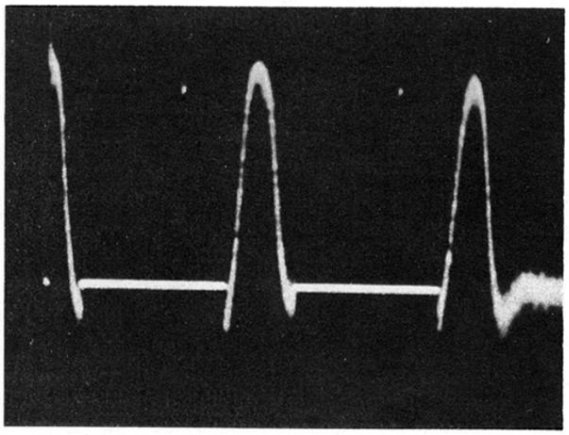

FIG. 8. Double-echo version of the experiment in Fig. 4 using pulse sequence 1(d) with $t_B = 180$ μsec. This shows that an extension of our echoes analogous to that of Carr and Purcell is possible.

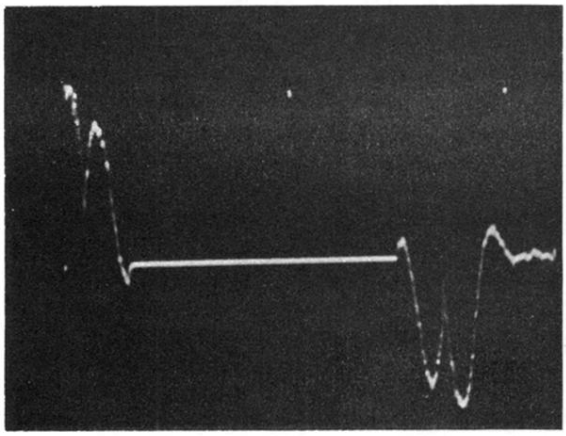

FIG. 9. Time reversal of a two-pulse experiment, using the pulse sequence in Fig. 1(e) with $\theta = 90°$. The first two pulses bring about a free induction decay and "solid echo." The following rf burst reverses this total sequence and then propagates it further backwards in time leading to the ensuing "mirror image" of the "solid-echo" experiment when the burst is terminated. The negative value of the "mirror image" is explained in the text. For this experiment $2t_{B1} + t_{B2} = 342$ μsec, corresponding to the noise-free portion of the trace.